Hindawi
International Journal of Antennas and Propagation
Volume 2021, Article ID 9913822, 10 pages
https://doi.org/10.1155/2021/9913822

Research Article

Bandwidth Enhancement of a Microstrip-Line-Fed Printed Rotated Wide-Slot Antenna Based on Self-Shape Blending Algorithm

Aiting Wu, Furan Zhu, Pengquan Zhang, Zhonghai Zhang, and Boran Guan

College of Electronics and Information, Hangzhou Dianzi University, No. 1158, 2nd Street, Xiasha District, Hangzhou 310018, China

Correspondence should be addressed to Pengquan Zhang; zhpq1999@163.com

Received 24 March 2021; Revised 16 July 2021; Accepted 12 August 2021; Published 19 August 2021

Academic Editor: Raffaele Solimene

This paper proposes a self-shape blending algorithm to improve antenna bandwidth. A printed antenna is designed for bandwidth enhancement based on the proposed algorithm; this approach can also be used to enhance bandwidth in other applications. The antenna completely covers WLAN bands and WiMAX bands after the proposed algorithm is applied. The shape of the rotating slot and the parasitic patch also changes, which excites additional resonance and improves the impedance matching at high frequencies. Test results show that the proposed antenna can work from 2.07 GHz to 5.94 GHz with $S_{11} \leq -10$dB. Compared to a slot antenna without the self-shape blending algorithm, the bandwidth increases by more than 0.7 GHz.

1. Introduction

Miniaturized and broadband slot antenna designs [1] have grown popular alongside the increased prevalence of wireless communication technology in recent years. The bandwidth of the microstrip antenna must be improved to make it suitable for wireless communication applications. This paper proposes a self-shape blending algorithm to improve the antenna bandwidth. The proposed algorithm is more convenient than the existing bandwidth improvement techniques and can be extended to a wider variety of antennas.

The microstrip wide-slot antenna is low cost, has a wide band, and can be readily integrated into single-chip equipment. Many researchers have explored the bandwidth expansion of miniaturized microstrip slot antennas. For example, the antenna bandwidth can be increased up to three times by adding square patches to the traditional L-shaped feed [2]. The bandwidth of a microstrip patch antenna can be increased over three times by introducing a fractal gap [3]. The bandwidth of a microstrip slot antenna with an etched fractal slot reaches up to 2.4 GHz [4]. A circular slot is added to a printed slot antenna to increase its bandwidth by more than 158% [5]. The bandwidth of a microstrip feed antenna can be increased by more than 100%, and the radiation mode can be enhanced, by choosing an appropriate feed shape in parallel with the slot shape [6]. The microstrip antenna with a rotating slot has shown a four-fold improvement in bandwidth over the traditional design, at up to 2.2 GHz [7]. Parasitic patches [8] can be added to the rotating-slow microstrip antenna [7] to further improve its impedance bandwidth from 1.80–6.09 GHz. Placing a parasitic slot-shaped patch into the middle of a printed antenna can further increase the bandwidth from 2.23 to 5.53 GHz [9]. Tuning stubs [10] are optimized to further improve the bandwith based on the antenna design in [9]. Different shapes of the tuning stubs are investigated in [11] to generate a series of different bandwidths. Many automated design methods and optimization algorithms are proposed and introduced into the antenna design. The animal migration optimization (AMO) algorithm [12] is used to optimize antenna designs. In [13], the generic algorithm (GA) is used to optimize the patch antenna. The particle swarm optimization (PSO) is introduced in [14] to

enhance a spline-shaped UWB antenna. The shape blending algorithm is proposed in [15, 16], blending two shapes to develop the patch of a printed CPW antenna, which obtains a UWB bandwidth. Compared with the conventional antenna design and bandwidth expansion methods, the design process using the optimization algorithms requires much less antenna design skills and expertise of the designer and is extensible to more different types of antenna.

A self-shape blending algorithm is developed in this paper to improve the antenna bandwidth. Compared with antennas with similar geometry [7, 9], the bandwidth of the antenna using self-shape blending algorithm is improved. And, the proposed method has the same advantage of the optimization algorithms. On the other side, compared with the basic shape blending algorithm, the self-shape blending algorithm does not need to find different shapes for the source and the target. Compared with the antenna in [9], the proposed method increases the bandwidth from 3.11 GHz (2.26–5.37 GHz) to 3.53 GHz (2.38–5.91 GHz) based on simulation results. Measured results show that the antenna bandwidth can reach up to 3.87 GHz (2.07–5.94 GHz).

2. Self-Shape Blending Algorithm

Self-shape blending originates from shape blending. Shape blending fuses the source shape and the target shape; the target shape of the self-shape blending algorithm is the same as the source shape.

The self-shape blending algorithm fuses its own points together. The specific steps are as follows:

(1) Select a shape for both source and target

(2) Select a series of points on the source shape and another series on the target shape

(3) Determine the corresponding rules of the points

(4) Fuse each pair of the corresponding points

Here is a concrete example of the self-shape blending process. The first step is to select a series of points on the source shape, as shown in Figure 1(a): A_1–A_8 and B_1–B_8 are chosen as the points of the target shape. A_1 corresponds to point B_1, A_2 corresponds to B_2,. . ., A_8 corresponds to B_8. Linear interpolation is used to blend each pair of the corresponding points, so we got the blended result $C(t)$ as

$$\begin{aligned} C(t) &= (1-t)*A + t*B, \\ &= \left[(1-t)*A_1 + t*B_1, \ldots\ldots, (1-t)*A_n + t*B_n\right], \\ &= \left[(1-t)*A_1 + t*A_2, \ldots\ldots, (1-t)*A_n + t*A_1\right], \\ &= \left[C_1(t), \ldots\ldots, C_2(t)\right]. \end{aligned} \tag{1}$$

3. Antenna Design

The antenna proposed in this paper is based on a reference antenna [9] with the structure shown in Figure 2. The shape of the reference antenna was changed here using the self-shape blending algorithm to improve its bandwidth and then compared against the reference antenna to observe its performance. The source shapes were determined by reference to previous studies. The shape of patch and slot of the microstrip antenna both affect the bandwidth, so the shape of the patch and slot can be optimized simultaneously.

We applied the self-shape blending algorithm to design the patch and slot shapes of the antenna as marked with double-diamonds in Figure 3. The relationship and path between vertices were determined according to which source shape corresponds to the target shape. Vertex correspondence uses this path to find the corresponding points of the source shape and the target shape. The corresponding points are fused. The generated point after fusion is the point of the new figure, which produces a series of antenna shapes. The points we used here are all points in the same graph. The second point in graph 1 is the first point of graph 2, and the subsequent points are analogous. The principle is shown in Figure 4, where A_1–A_8 correspond to B_1–B_8 and D_1–D_8 correspond to E_1–E_8.

The vertex path problem was next solved by linear interpolation. Same as the example described in the previous section, $C(t)$ is the self-blended result of $A(t)$ and $B(t)$, and $F(t)$ is the self-blended result of $C(t)$ and $D(t)$, as expressed in the following two equations:

$$\begin{aligned} C(t) &= (1-t)*A + t*B, \\ &= \left[(1-t)*A_1 + t*B_1, \ldots\ldots, (1-t)*A_n + t*B_n\right], \\ &= \left[(1-t)*A_1 + t*A_2, \ldots\ldots, (1-t)*A_n + t*A_1\right], \\ &= \left[C_1(t), \ldots\ldots, C_2(t)\right], \\ F(t) &= (1-t)*D + t*E, \\ &= \left[(1-t)*D_1 + t*E_1, \ldots\ldots, (1-t)*D_n + t*E_n\right], \\ &= \left[(1-t)*D_1 + t*D_2, \ldots\ldots, (1-t)*D_n + t*D_1\right], \\ &= \left[F_1(t), \ldots\ldots, F_2(t)\right], \end{aligned} \tag{2}$$

where $n = 8$. $C(t)$ is used as the shape of the slot and $F(t)$ is used as the shape of the parasitic patch. A and D represent the collection of points of the source shape, B and E represent the collection of points of the target shape, and t is the coefficient of shape blending.

As shown in Figure 5, a series of the antenna form was obtained with a constantly changing t value.

Figure 6(a) show the geometry of the reference antenna [9] and proposed antenna. Figure 6(b) shows a photograph of the reference antenna and Figure 6(b) shows a photograph of the manufactured antenna (scale = mm).

Both antennas were designed on a substrate with $\varepsilon_r = 4.4$, $\tan\delta = 0.02$, and height of 1.6 mm. The substrate size is 37 mm × 37 mm. A new rotating slot and rotating patch were added to the reference antenna [9] by the self-shape blending algorithm. The parasitic patch and slot are rotated squares based on the reference structure [9]. All metal parts were made of copper with 0.05 mm thickness. An ideal conductor (PEC) was also used in the simulation, which was conducted by the finite element method (FEM) HFSS15. The dimensions of the antenna are listed in Table 1.

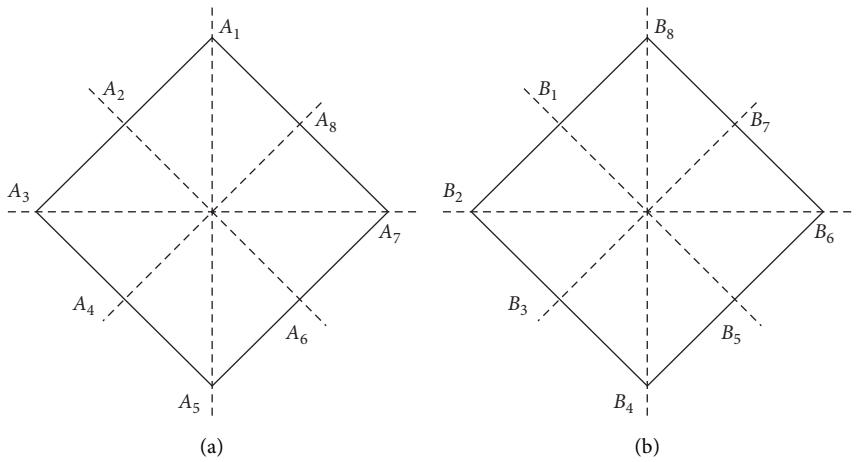

FIGURE 1: Self-shape fusion diagram: (a) source shape and (b) target shape.

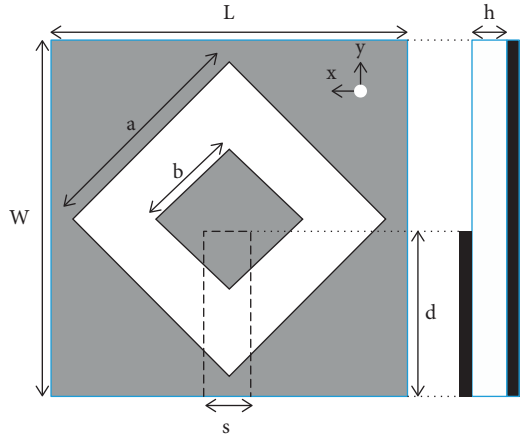

FIGURE 2: Geometry of reference antenna.

Compared with the traditional microstrip wide-slot antenna, the antenna bandwidth can be improved by adding a rotating slot shape [7]. Compared with the microstrip wide-slot antenna [7], the bandwidth can be further improved by embedding a parasitic patch into the center of the rotated square slot [9]. Compared with the microstrip wide-slot antenna [9], the bandwidth was even further improved in this study by changing the shape of the parasitic patch and rotating the square slot by the self-shape blending algorithm.

4. Results and Discussion

Different t values can have different patch and slot shapes. In other words, t values give rise to different antenna structures. The antennas we simulated with different t values are shown in Figure 7.

As t values change and thus different antenna shapes are created, a series of S_{11} also forms. When $t = 0$, the antenna has the source shape and its bandwidth is 2.26–5.37 GHz. When $t = 0.1$, the antenna patch and slot shapes change and a new resonance mode appears which increases the bandwidth to 2.32–5.59 GHz. When $t = 0.2$, the antenna patch and slot shapes continue to change and the new resonant mode is close to the existing resonant mode; the two resonant modes are fused to produce wider bandwidth up to 2.38–5.91 GHz. When $t = 0.3$, the fusion of the two resonant modes begins to deteriorate and the bandwidth is divided into two segments, 2.48–3.81 GHz and 4.84–5.99 GHz. When $t = 0.4$, the fusion situation further deteriorates and the bandwidth is completely divided into two disparate segments, 2.51–3.49 GHz and 5.12–5.99 GHz.

The current distribution of the antenna at the frequencies of 2.7 GHz and 5.76 GHz is shown in Figure 8. Figures 8(a) and 8(c) show the original antenna, while Figures 8(b) and 8(d) show the final, optimized antenna. The surface current of the parasitic patch obtained in this study was markedly enhanced compared with that of the reference antenna [9]. This also indicates that the coupling between the feeder and parasitic patch was enhanced due to changes in the parasitic patch and gap. The coupling-related enhancement further improved the antenna matching and bandwidth characteristics. The surface current distribution of other frequencies appears to be similar at low frequencies (Figure 8(b)) and high frequencies (Figure 8(d)).

The antenna results of S_{11} are shown in Figure 9. The original antenna had $t = 0$. The final simulation antenna

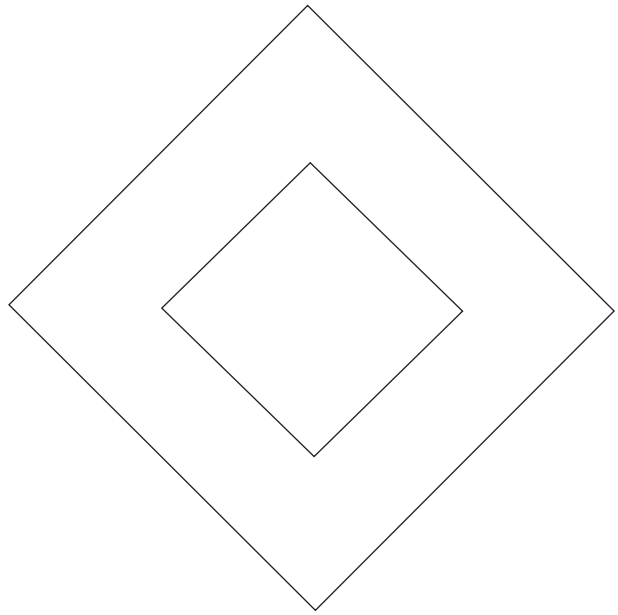

Figure 3: Source shape (target shape).

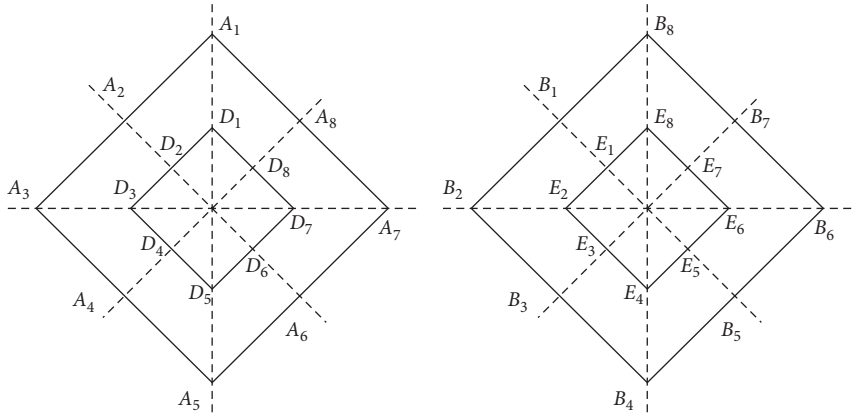

Figure 4: Finding vertex correspondence. (a) Graph 1 (source shape). (b) Graph 2 (target shape).

was obtained at $t = 0.2$ with bandwidth of 3.53 GHz (2.38–5.91 GHz). The final antenna bandwidth measurement was 3.87 GHz (2.07–5.94 GHz); the simulated bandwidth of the original antenna was 3.11 GHz (2.26–5.37 GHz) and the measured bandwidth of the original antenna was 3.09 GHz (2.38–5.47 GHz). The antenna was fabricated using the dimensions in Figure 6(a). The measurement and simulation results are in accordance but do show some error, which we mainly attribute to the manufacturing process having failed to produce a structure with exactly the same shape as the simulation. Additionally, there were defects in the SMA and welding joints in the structure we subjected to measurement.

The instrument we used for bandwidth measurements is a vector network analyzer (VNA) (Figure 10). The radiation parameters of the antenna were tested in a test chamber (Figure 11).

The normalized radiation patterns at 2.7 GHz and 5.76 GHz are shown in Figure 12. The radiation pattern on the E plane (x-z plane) is almost bidirectional in Figures 12(a) and 12(c). The radiation pattern on the H plane (y-z plane) maintains significant omnidirectional characteristics throughout the frequency band in Figures 12(b) and 12(d). The measurements show that the radiation characteristics of the proposed antenna are similar to those of the reference antenna [7, 9]. Figure 13 shows where the measured absolute gain is about 2.5–4.65 dBi in the range of 2000–2700 MHz, about 4.64–4.65 dBi in the range of 2700–5000 MHz, and about 2.9–4.64 dBi in the range of 5000–5940 MHz. The measurement and simulation results are in accordance and, again, the proposed antenna performed similarly to the reference antenna [9].

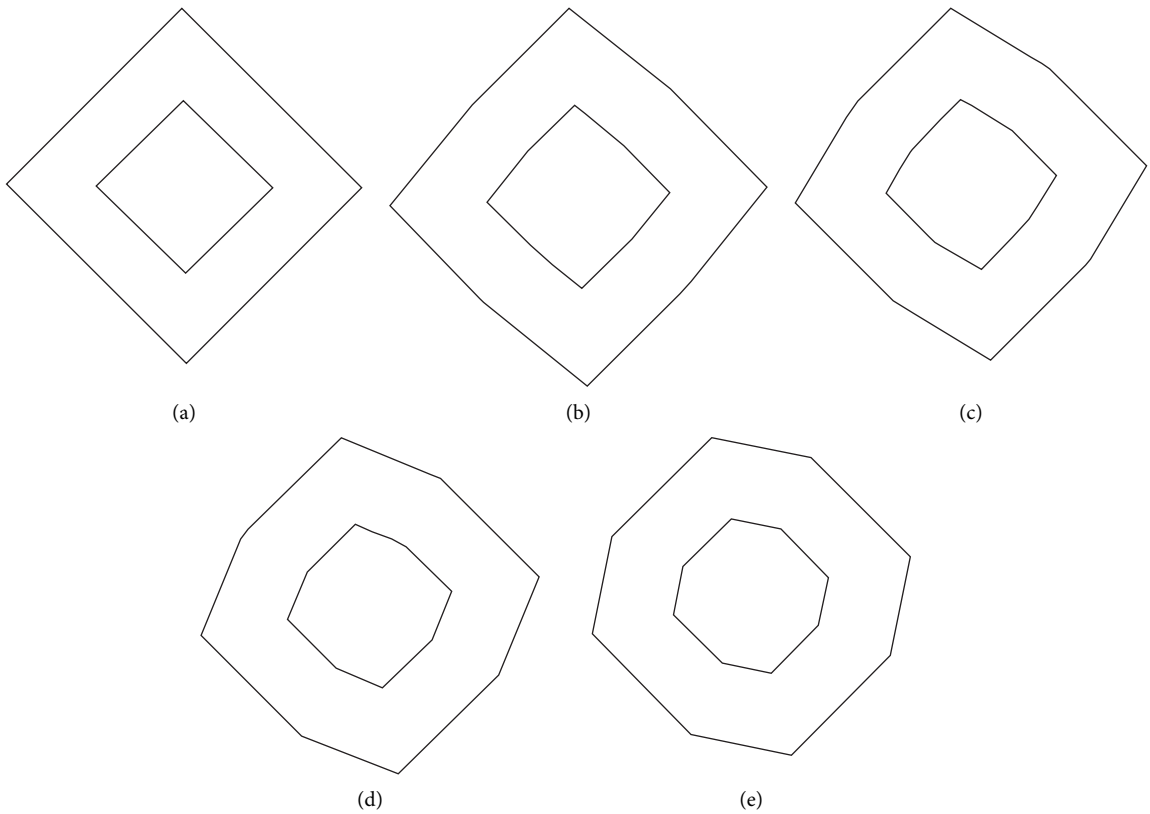

Figure 5: Blended shapes: (a) $t = 0$, (b) $t = 0.1$, (c) $t = 0.2$, (d) $t = 0.3$, and (e) $t = 0.4$.

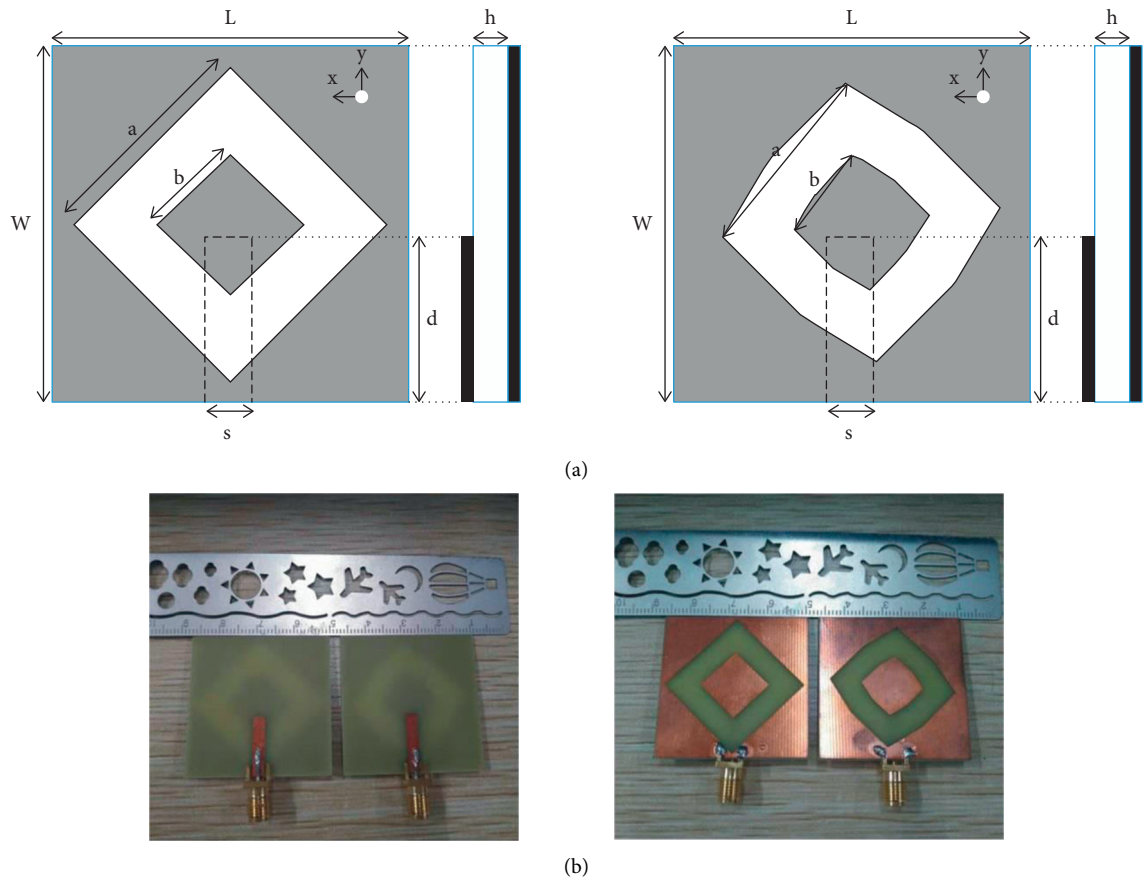

Figure 6: (a) Reference antenna structure and (b) proposed antenna structure.

Table 1: Dimensions of the proposed antenna.

Parameters	W	L	h	a	b	d	s
Dimensions (mm)	37	37	1.6	24.7	12	15	3

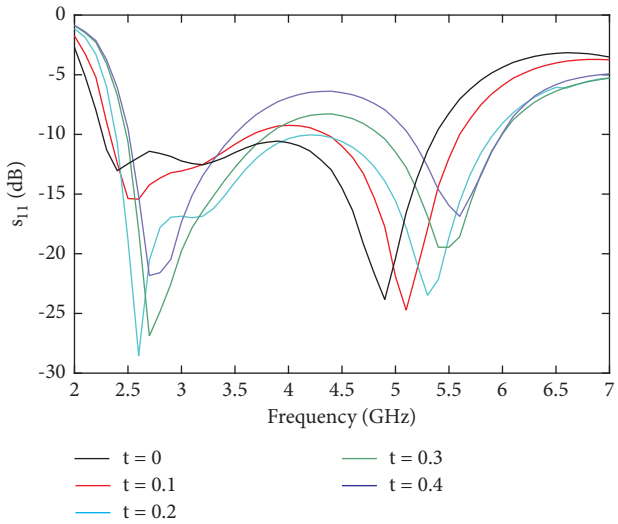

Figure 7: S_{11} results with different t values.

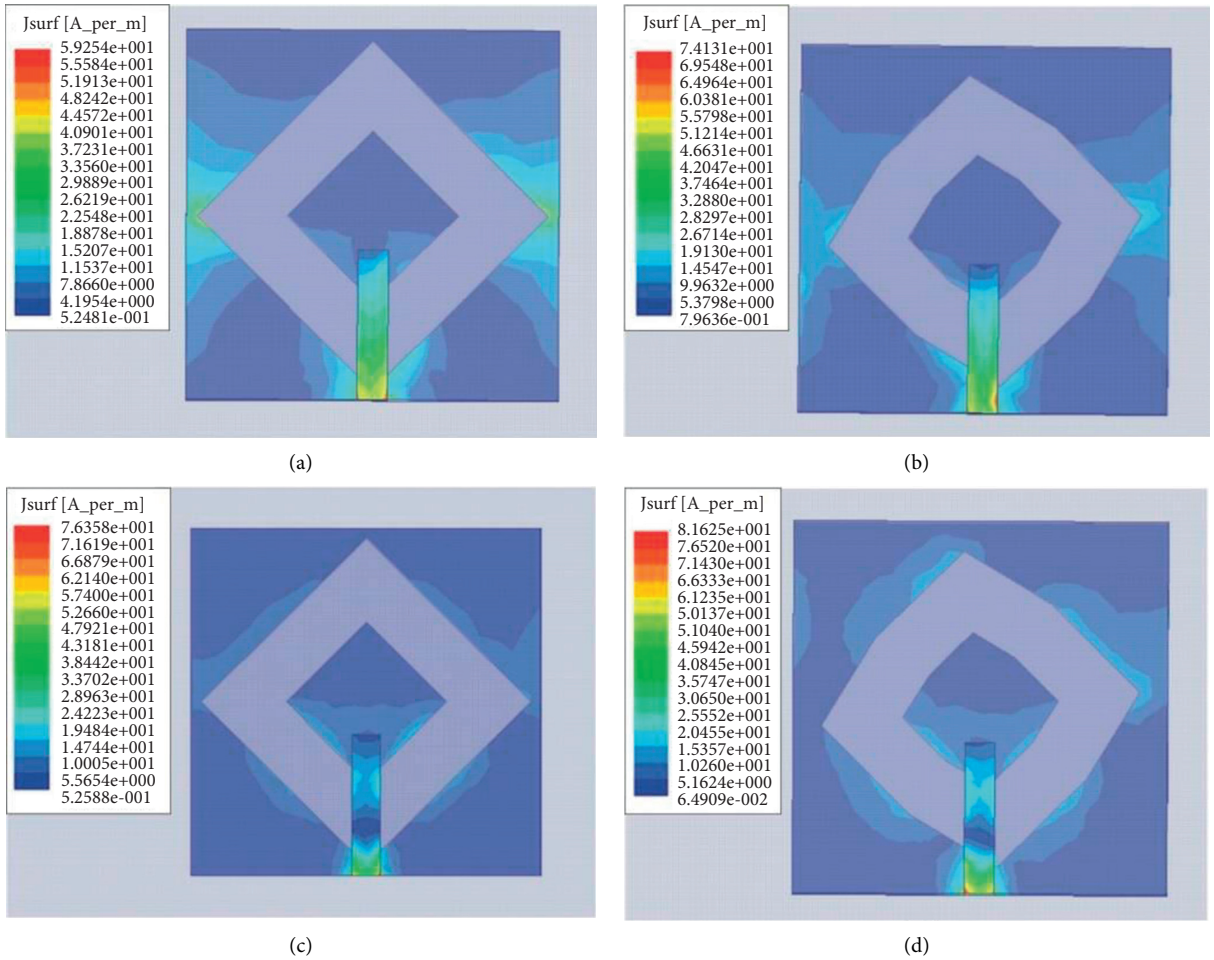

Figure 8: Surface current distribution of antenna. (a) Original antenna at 2.7 GHz, (b) final antenna at 2.7 GHz, (c) original antenna at 5.76 GHz, and (d) final antenna at 5.76 GHz.

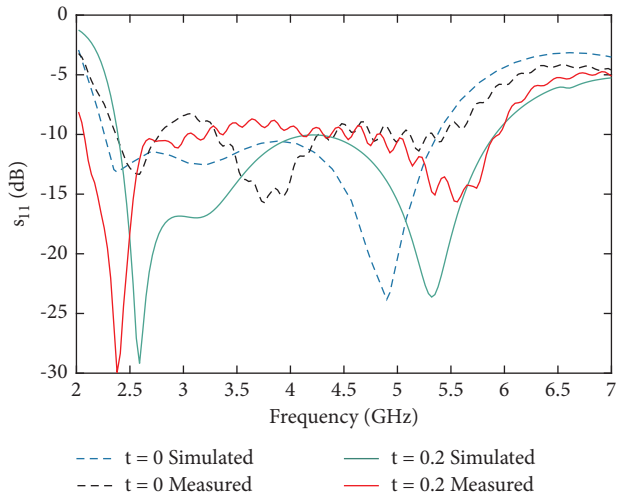

Figure 9: Simulated and measured antenna S_{11} values.

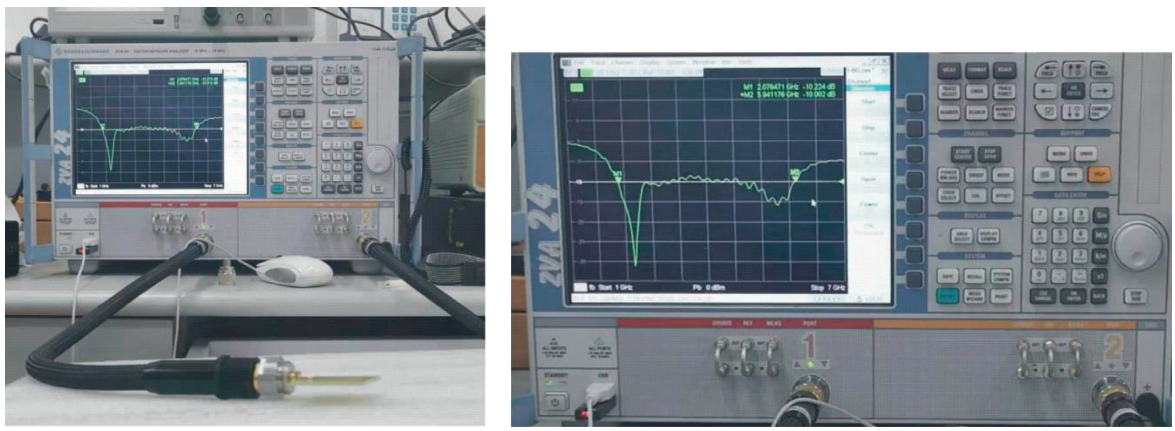

Figure 10: Photograph of VNA

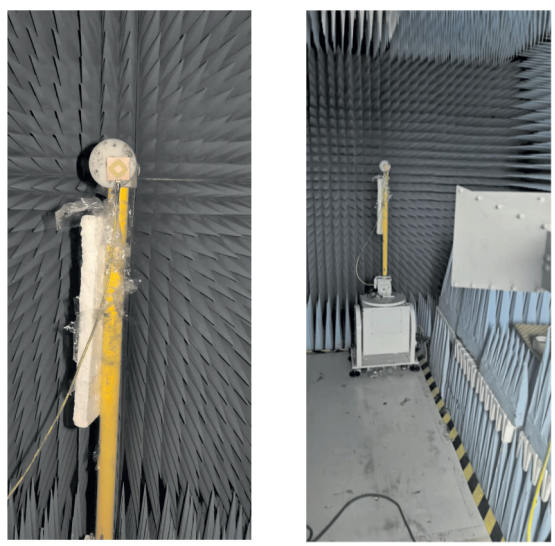

Figure 11: Photograph of the test chamber.

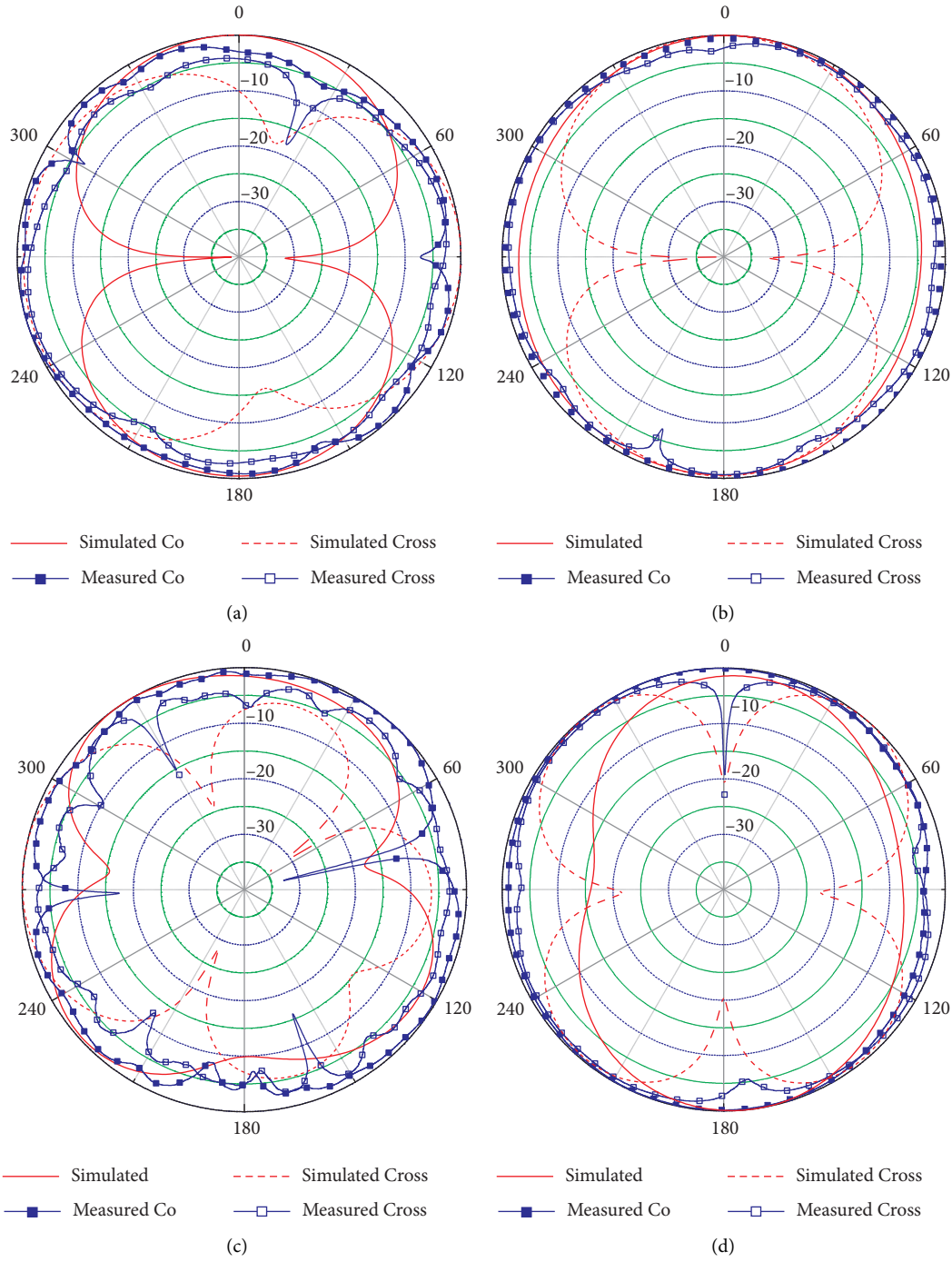

Figure 12: Radiation patterns of antenna: (a) E plane at 2.7 GHz, (b) H plane at 2.7 GHz, (c) E plane at 5.76 GHz, and (d) H plane at 5.76 GHz.

Compared with other approaches to bandwidth improvement [7, 9, 17, 18], the proposed method is more applicable to a wider variety of antennas. And, compared with many literatures on bandwidth improvement in recent years, the bandwidth improvement of the antenna in this paper is more. As in [7, 9, 19–22], the proposed method is also effectively independent of the antenna theory and can markedly improve existing antenna designs (Table 2).

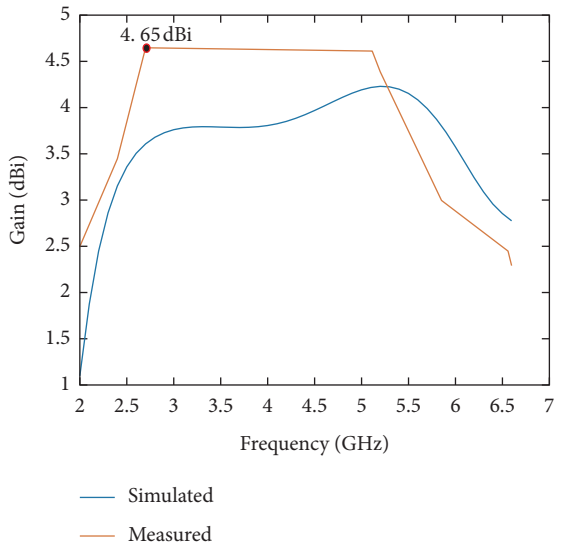

Figure 13: Simulated and measured absolute gain results.

Table 2: Comparison between the proposed antenna with the recent works.

References	Novelty	Antenna design	Bandwidth	Gain
[7]	Printed antenna fed by a microstrip line with a rotated slot for bandwidth enhancement	Dependent on antenna theory	3400–5600 MHz	3400–5600 MHz 3–5.2 dBi
[9]	Printed wide slot antenna with a parasitic patch for bandwidth enhancement	Dependent on antenna theory	2230–5350 MHz	2230–5350 MHz 3.5–5 dBi
[17]	Pair of tuning stubs attached to the feedline for bandwidth enhancement	Dependent on antenna theory	2380–9640 MHz	2380–9640 MHz 0.5–4.5 dBi
[18]	Rectangular slots cut into the square patch for bandwidth enhancement	Dependent on antenna theory	1130–9350 MHz	No relevant data available
[19]	By introducing diamond shaped slot and ring in patch and defected ground structure	Dependent on antenna theory	10000–10512 MHz	10000–10512 MHz 7.9 dBi
[20]	By adding the split ring resonator (SRR) metamaterial	Dependent on antenna theory	5500–6500 MHz	5500–6500 MHz 2-5 dBi
[21]	New feeding scheme of short-circuited CPW feed with a length of one wavelength is utilized for bandwidth enhancement	Dependent on antenna theory	2420–2510 MHz	2420–2510 MHz. 0.5-3 dBi
[22]	By introducing *T* shaped slot	Dependent on antenna theory	3300–3400 MHz	3320–3370 MHz 5.88–5.9 dBi
This paper	Self-shape blending algorithm for bandwidth enhancement in various antennas	Independent of antenna theory	2070–5940 MHz	2070–5940 MHz 3–4.65 dBi

5. Conclusions

This paper proposes a self-shape fusion algorithm for antenna bandwidth enhancement. This method can be used to improve the bandwidth of various types of antenna. A microstrip slot antenna based on the proposed algorithm was developed to test its feasibility and effectiveness. The self-shape blending algorithm improves the antenna's operating bandwidth by importing extraresonances. The proposed antenna has a wider bandwidth than a similar reference antenna [9].

Data Availability

The data used to support the finding of this study are included within the article.

Conflicts of Interest

The authors declare that they have no conflicts of interest regarding the publication of this paper.

Acknowledgments

This work was supported by the National Natural Science Foundation of China (Grant nos. 61501153 and 61801153), the State Key Laboratory of Millimeter Waves (Grant no. K202012), and the Natural Science Foundation of Zhejiang Province (Grant no. LQY20F010001).

References

[1] A. A. Deshmukh and K. P. Ray, "Compact broadband slotted rectangular microstrip antenna," *IEEE Antennas and Wireless Propagation Letters*, vol. 8, pp. 1410–1413, 2009.

[2] Y. Sung, "A printed wide-slot antenna with a modified L-shaped microstrip line for wideband Applications," *IEEE Transactions on Antennas and Propagation*, vol. 59, no. 10, pp. 3918–3922, 2011.

[3] H. Dholakiya, D. Pujara, and S. B. Sharma, "Wide-slot fractal antenna design with improved bandwidth," in *Proceeding of Applied Electromagnetics Conference (AEMC)*, Kolkata, India, December 2011.

[4] W. L. Chen, G. Wang, and C. X. Zhang, "Bandwidth enhancement of a microstrip-line-fed printed wide-slot antenna with a fractal-shaped slot," *IEEE Transactions on Antennas and Propagation*, vol. 57, no. 7, pp. 2176–2179, 2009.

[5] S.-W. Qu, C. Ruan, and B.-Z. Wang, "Bandwidth enhancement of wide-slot antenna fed by CPW and microstrip line," *IEEE Antennas and Wireless Propagation Letters*, vol. 5, pp. 15–17, 2006.

[6] Y. F. Liu, K. L. Lau, Q. Xue, and Chan, "Experimental studies of printed wide-slot antenna for wide-band applications," *IEEE Antennas and Wireless Propagation Letters*, vol. 3, pp. 273–275, 2004.

[7] J.-Y. Jan and J. W. Jia, "Bandwidth enhancement of a printed wide-slot antenna with a rotated slot," *IEEE Transactions on Antennas and Propagation*, vol. 53, no. 6, pp. 2111–2114, 2005.

[8] J.-Y. Jan and L.-C. Wang, "Printed wideband rhombus slot antenna with a pair of parasitic strips for multiband applications," *IEEE Transactions on Antennas and Propagation*, vol. 57, no. 4, pp. 1267–1270, 2009.

[9] Y. Sung, "Bandwidth enhancement of a microstrip line-fed printed wide-slot antenna with a parasitic center patch," *IEEE Transactions on Antennas and Propagation*, vol. 60, no. 4, pp. 1712–1716, 2012.

[10] O. G. Kwame, W. Guang, X. X. Ling et al., "Bandwidth enhancement of a microstrip-line-fed printed rotated wide slot antenna with tuning stubs," in *Proceeding of the 2016 IEEE MTT-S International Wireless Symposium (IWS)*, Shanghai, China, October 2016.

[11] X. L. Liang, T. A. Denidni, L. N. Zhang, R.-H. Jin, J.-P. Geng, and Q. Yu, "Printed binomial-curved slot antennas for various wideband applications," *IEEE Transactions on Microwave Theory and Techniques*, vol. 59, no. 4, pp. 1058–1065, 2011.

[12] E. D. Ülker and S. ülker, "Antenna design using animal migration optimisation algorithm," *Journal of Engineering*, vol. 2016, no. 8, pp. 298–301, 2016.

[13] M. John and M. J. Ammann, "Wideband printed monopole design using a genetic algorithm," *IEEE Antennas and Wireless Propagation Letters*, vol. 6, pp. 447–449, 2007.

[14] L. Lizzi, F. Viani, R. Azaro, and A. Massa, "Optimization of a spline-shaped UWB antenna by PSO," *IEEE Antennas and Wireless Propagation Letters*, vol. 6, pp. 182–185, 2007.

[15] A. Wu, B. Guan, and Z. Zhang, "A wideband printed slot antenna using shape blending," in *Proceeding of the 2016 11th International Symposium on Antennas, Propagation and EM Theory (ISAPE'16)*, pp. 92–94, Guilin, China, October 2016.

[16] A. Wu, B. Guan, and Z. Zhang, "Wideband printed antenna design using a shape blending algorithm," *International Journal of Antennas and Propagation*, vol. 2017, pp. 1–8, Article ID 9073765, 2017.

[17] O. G. Kwame, W. Guangjun, X. X. Lin, and M. A. Basit, "Bandwidth enhancement of a microstrip-line-fed printed rotated wide slot antenna with tuning stubs," in *Proceedings of the 2016 IEEE MTT-S International Wireless Symposium (IWS)*, Shanghai, China, March 2016.

[18] R. Jabeen and G. S. Tripathi, "Realization of printed rotated slot antenna with tuning stubs fed by microstrip feedline for bandwidth enhancement," in *Proceedings of the 2018 3rd International Conference on Internet of Things: Smart Innovation and Usages (IoT-SIU)*, Bhimtal, India, November 2018.

[19] T. F. A. Nayna, F. Ahmed, and E. Haque, "Bandwidth enhancement of a rectangular patch antenna in X band by introducing diamond shaped slot and ring in patch and defected ground structure," in *Proceedings of the 2017 International Conference on Wireless Communications, Signal Processing and Networking (WiSPNET)*, Chennai, India, March 2017.

[20] N. Ulfah and T. Hariyadi, "Design of horizontal polarization microstrip patch antenna with bandwidth enhancement at C-band frequency," in *Proceedings of the 2020 Third International Conference on Vocational Education and Electrical Engineering (ICVEE)*, Surabaya, Indonesia, October 2020.

[21] C. Chu, Y. Zhu, and J. Wang, "A CPW-fed patch antenna with low profile and bandwidth enhancement," in *Proceedings of the 2019 International Conference on Microwave and Millimeter Wave Technology (ICMMT)*, Guangzhou, China, May 2019.

[22] D. W. Astuti, F. Y. Zulkifli, and E. T. Rahardjo, "Bandwidth enhancement of substrate integrated waveguide cavity antenna using T-backed slot," in *Proceedings of the 2019 IEEE Conference on Antenna Measurements & Applications (CAMA)*, Kuta, Bali, Indonesia, October 2019.